Italian Journal of Food Science, 2024; 36 (3): 184–202

Chamuangone-rich rice bran oil ameliorates neurodegeneration in $AlCl_3$/D-galactose model *via* modulation of behavioral, biochemical, and neurochemical parameters

Badriyah S. Alotaibi[1], Uzma Saleem[2]*, Maryam Farrukh[3], Sadaf Waseem[3], Zunera Chauhdary[3], Ifat Alsharif[4], Wedad Saeed Alqahtani[5], Abdullah R. Alanzi[6], Mona N. BinMowyna[7], Muhammad Ajmal Shah[8,9]*, Khairul Anam[9], Yasmene F. Alanazi[10], Abdulelah M. Almuwallad[11], Abdulmajid M. Almuwallad[11], Pharkphoom Panichayupakaranant[12]*, Ana Sanches Silva[13–15]*

[1]Department of Pharmaceutical Sciences, College of Pharmacy, Princess Nourah bint Abdulrahman University, P.O. Box 84428, Riyadh 11671, Saudi Arabia; [2]Punjab University College of Pharmacy, University of the Punjab, Lahore, Pakistan; [3]Department of Pharmacology, Faculty of Pharmaceutical Sciences, Government College University, Faisalabad, Pakistan; [4]Department of Biology, Jamoum University College, Umm Al-Qura University, Makkah, Saudi Arabia; [5]King Abdullah International Medical Research Center (KAIMRC), King Saud Bin Abdulaziz University for Health Sciences (KSAU-HS), MNGHA, Saudi Arabia; [6]Department of Pharmacognosy, College of Pharmacy, King Saud University, Riyadh, Saudi Arabia; [7]College of Education, Shaqra University, Shaqra, Saudi Arabia; [8]Department of Pharmacy, Hazara University, Mansehra, Pakistan; [9]Department of Pharmacy, Faculty of Medicine, Diponegoro University, Jl. Prof. Mr. Sunario, Tembalang, Semarang, Central Java, Indonesia; [10]Department of Biochemistry, Faculty of Science, University of Tabuk, Tabuk, Saudi Arabia; [11]Department of Medical Laboratory Technology, Faculty of Applied Medical Sciences, King Abdulaziz University Hospital, Jeddah, Saudi Arabia; [12]Department of Pharmacognosy & Pharmaceutical Botany, Faculty of Pharmaceutical Sciences, Prince of Songkla University, Hat Yai, Thailand; [13]University of Coimbra, Faculty of Pharmacy, Polo III, Azinhaga de Stª Comba, Coimbra, Portugal; [14]Centre for Animal Science Studies (CECA), ICETA, Porto, Portugal; [15]Associate Laboratory for Animal and Veterinary Sciences (Al4AnimalS), Lisbon, Portugal

***Corresponding Authors:** Uzma Saleem, Punjab University College of Pharmacy, University of the Punjab, Lahore 54000, Pakistan. Email: uzma95@gmail.com; Muhammad Ajmal Shah, Department of Pharmacy, Hazara University, Mansehra, Pakistan. Email: ajmalshah@hu.edu.pk; Pharkphoom Panichayupakaranant, Department of Pharmacognosy & Pharmaceutical Botany, Faculty of Pharmaceutical Sciences, Prince of Songkla University, Hat Yai, Thailand. Email: pharkphoom.p@psu.ac.th; Ana Sanches Silva, Faculty of Pharmacy, University of Coimbra, Polo III, Azinhaga de Stª Comba, Coimbra 3000-548, Portugal. Email: asanchessilva@ff.uc.pt

Received: 15 May 2024; Accepted: 3 July 2024; Published: 22 July 2024

PAPER

Abstract

Chamuangone is an exotic medicinal compound isolated from *Garcinia cowa* leaves. It shows great potential against inflammation, neurodegeneration, and oxidation. Through green extraction method, chamuangone-rich rice bran oil (CRBO) containing 1.97 mg/mL of chamuangone was obtained. This research study investigates the therapeutic effects of CRBO on D-galactose- and aluminum chloride ($AlCl_3$)-induced Alzheimer's disease in rat model. In all, 30 rats were divided into six groups and treated for 42 days as follows: control group (vehicle), disease control group ($AlCl_3$ 150 mg/kg + D-galactose 150 mg/kg p.o.), standard group (rivastigmine 3 mg/kg p.o.), and CRBO treatment groups with doses of 2.5, 5.0, and 7.5 mg/kg p.o. Neurobehavioral studies were performed on completion of 42 days. Furthermore, biochemical, neurochemical, and histopathological analyses were performed. CRBO treatment mitigated impairment in neuromuscular coordination, mentation and cognition in behavioral tasks. It potentially recovered ($p < 0.001$) the declined level of catalase, superoxide dismutase, reduced glutathione and lipid peroxidation. Neurochemical analysis revealed the restoration of serotonin, noradrenaline, and dopamine concentration in the brain after CRBO treatment. Histopathological examination of vital organs revealed recovery in CRBO-treated rats in a dose-dependent manner. Owing to neurotoxic effects of inducing

 ISSN 1120-1770 online, DOI 10.15586/ijfs.v36i3.2643

agents, the level of acetylcholinesterase decreased in disease control group; however, CRBO treatment recovered the declined activity of this enzyme. Therefore, it is concluded that CRBO significantly recovered the neurodegenerative effects through multiple pathways, such as amelioration of oxidative stress and neuronal plasticity. Therefore, this innovative green remedy can be considered as a natural alternative for treating neurodegenerative disorders.

Keywords: Alzheimer's disease; animal behavior; chamuangone-rich rice bran oil, neurochemical analysis; neuroinflammation, phytomedicine

Introduction

Loss of neurons in motor, sensory, or cognitive regions of the brain is usually selective and symmetrical in many neurodegenerative disorders. They are characterized by cell loss patterns and the discovery of cellular markers specific to diseases (Martin, 1999). The most prevalent form of dementia that develops in mid-to-late life is Alzheimer's disease (AD), a complicated and profoundly diverse medical condition (Sisodia, 1999). Approximately 5 million new cases of dementia are discovered every year, affecting over 24 million individuals worldwide, the majority of whom have AD (Qiu *et al.*, 2022). The earliest stage in AD is mild, and there are no clear indications that could make way for a timely diagnosis prior to irreversible abnormalities (Förstl and Kurz, 1999). Decline in cognition, diminished routine tasks of everyday life, and accompanying behavioral problems are manifested at early stages (Shin *et al.*, 2005). In moderate to mild conditions, severe depression is linked with apathy, difficulty in sleeping, negative mood, feelings of low self-worth, nervousness, and despair. In severe condition, likelihood of reduced severe depression is observed, while agitation, psychosis, and aggression are increased (Lopez *et al.*, 2003).

Alzheimer's disease is an age-related neurodegenerative condition described clinically by an ongoing decrease in cognitive capacity whereas formation of senile plaques, neurofibrillary tangles (NFTs), and neuronal degeneration in specific brain areas is the pathological explanation (Kim and Tsai, 2009). Cortex, entorhinal cortex (EC), hippocampus, ventral striatum, and cerebral cortex of the brain are the most affected parts (Hampel *et al.*, 2018). Reduced cholinergic activity in the brain of AD patients is prevalent whereas experimental research has demonstrated that acetylcholinesterase (AchE) has a vital role in learning and memory (Craig-Schapiro *et al.*, 2009). The basal forebrain complex's cholinergic neurons are described to suffer moderate degenerative alterations with aging. This results in cholinergic hypofunction, linked to the progression of memory problems with aging, causing observed deficits in cognition, thus contributing to the formation of cholinergic theories of memory dysfunction in geriatrics, leading to the formation of β-amyloid plaques (Schliebs and Arendt, 2006). Autophagy and mitochondrial dysfunction are initial and most promising factors in AD pathogenesis. Incomplete autophagy procedure imparts too many degraded macromolecules, which deposit in the brain and affects brain functioning (Tran and Reddy, 2021). Malfunctioning of mitochondria causes synapses to build up lipofuscin, which may worsen neuronal dysfunction (Moreira *et al.*, 2010).

Another main phenomenon in the pathophysiology of AD is oxidative stress, since the brain is more susceptible to oxidative stress than other organs. Most neuronal components (lipids, proteins, and nucleic acids) tend to be oxidized in AD due to mitochondrial malfunction, elevated metal levels, inflammation, and β-amyloid (Aβ) peptides (Chen and Zhong, 2014). AchE inhibitors are first-line treatment for AD and are linked to improve cognitive function, behavior, and activities of daily living. Memantine can also be used in combination with AchE inhibitors (Winslow *et al.*, 2011). Second-generation (atypical) antipsychotic medications are also frequently used for treating psychosis, aggression, and agitation in AD patients (Caraci *et al.*, 2020; Schliebs and Arendt, 2006). The 'disease-modifying' medications, having capability to treat AD at initial stages, are researched actively. To halt disease progression, these medications must delay pathological phases which trigger clinical symptoms, such as the formation of extracellular amyloid plaques and intracellular NFTs, inflammatory conditions, oxidative damage, iron deregulation, and cholesterol metabolism (Yiannopoulou and Papageorgiou, 2013). Herbal medicines have been used since ancient times to treat behavioral and psychological AD symptoms with varying degrees of success and fewer adverse effects. Although some US Food and Drug Administration (FDA)-approved therapies are available for managing AD, the results tend to be insufficient; thus herbal therapies have a significant role in treating AD (Jadhav *et al.*, 2019).

D-galactose, a brain sugar, is a source of energy for various processes. Recent studies have shown that certain diseases, such as AD, are induced by D-galactose

because it causes abnormal alterations in mitochondrial cells, along with the formation of oxidative free radicals, damaging neurons and causing dementia in experimental animals (Hua *et al.*, 2007). Aluminum chloride is also demonstrated to form twisted tangles resulting in AD (Kumar and Singh, 2015).

'Chamuang' is a Thai name of *Garcinia cowa*. It is an edible plant of the Clusiaceae family. This plant is a small to medium size tree of 30-m height. Its fruits having a nasty taste are consumed (Yorsin *et al.*, 2023). Parts of *Garcinia cowa* have many medicinal benefits. Many pharmacological attributes related to this plant are reported, such as antiviral, antidepressant, antifungal, antioxidant, anti-leishmaniases, antitumor, and anti-obesity properties. In many parts of the world, *Garcinia cowa* is used traditionally for improving blood circulation, as an expectorant, and for indigestion. Phloroglucinols, chamuangone, xanthones, cowaxanthone, flavonoids, and garcicowanone are the main phytoconstituents of the plant (Panichayupakaranant and Sakunpak, 2013). Polyoxygenated xanthones and garcicowanone manifested strong neuroprotective and antioxidant potential by prohibiting the synthesis of reactive oxygen species and reducing Ca^{+2} influx (Tran *et al.*, 2022).

Chamuangone manifested a potentially strong chemotherapeutic activity by constraining cell proliferation and prompting apoptosis in HeLa cell lines (Sae-Lim *et al.*, 2020); it also showed cytotoxic effects against lung leukemia and adenocarcinoma cell lines (Sakunpak *et al.*, 2017). Studies have demonstrated a substantial antibacterial property of active component chamuangone (Sakunpak and Panichayupakaranant, 2012). Using a green microwave-aided extraction method, chamuangone-rich rice bran oil (CRBO) was produced. It demonstrated strong anticancer activity against human cancer cell lines and was noninvasive to normal cells (Sae-Lim *et al.*, 2019b). In light of recently reported pharmacological activities of chamuangone (Alotaibi *et al.*, 2024), this study was planned to explore the neuroprotective potential of CRBO against D-galactose- and aluminum chloride-induced Alzheimer's rat model.

Materials and Methods

Provenance of chamuangone-rich rice bran oil

Green microwave-assisted extraction method was used to prepare standardized CRBO. The standardization was carried out by high-performance liquid chromatography (HPLC; 1.97 mg/mL) at Phytomedicine and Pharmaceutical Biotechnology Excellence Centre, Faculty of Pharmaceutical Sciences, Prince of Songkla University, Hat Yai, Songkhla, Thailand (Sae-Lim *et al.*, 2019a).

Animal husbandry

The experiment was conducted on 30 rats of either gender weighing 100–200 g. The rats were purchased from the animal house of Government College University, Faisalabad. They were kept in close supervision under ideal conditions (room temperature: 22 ± 3°C, humidity: 30–55%, and a 12-h dark and light cycle) for about 7 days prior to beginning the experiment to make animals sufficiently relaxed.

Study design

Six groups of mice were created (n = 5). Group 1 was the control group that received vehicle only. Group 2 was the disease control group that was administered aluminum chloride and D-galactose orally 150 mg/kg each. Group 3 was the standard group and administered 3 mg kg of oral rivastigmine. Groups 4–6 were CRBO-treated groups with CRBO oral doses of 2.5, 5.0, and 7.5 mg/kg. Behavioral changes in animals were studied by taking neurobehavioral observations on day 42 of the study. Blood was collected with the help of cardiac puncture for biochemical and hematological analyses. The animals were anesthetized by using 10% isoflurane. The brain, heart, kidney, liver, and lungs were excised by cervical dislocation for histopathological analysis. All vital organs were preserved in 10% formalin, while brain tissues were kept in ice-cold phosphate buffer for measuring neurotransmitters.

Neurobehavioral observations (Table S1)

Open field test

Different behaviors, such as movement and mental state of animals, were assessed with the help of open field test by measuring locomotion. The setup contained a square box having a field (60 × 60 cm) containing 36 squares (10 × 10 cm) enclosed by a wall of Plexiglas having 25-cm height. Of these 36 squares, 20 squares that were close to the wall was named 'peripheral field' and the rest of 16 squares was named 'closed field' squares. The animals were placed on a quadrant to discover field. Number of lines crossed, motility, scratching, and peripheral exploration were observed with the help of a camera (Chauhdary *et al.*, 2019).

Morris water maze test

This is a dimensional comprehension trial that requires navigating from points of origin along the shore of an unrestricted aquatic area to a hidden evacuation station employing peripheral stimuli (Vorhees and Williams, 2006). The apparatus for this test comprised a pool of water having a diameter of 1.5–2.0 m. The water was

treated with a substance that changed its appearance into an easily noticeable form. An escape object was placed in hiding sufficiently from the water surface to test the attributes related to the animal's motivation to escape, such as the distance covered and the swimming speed to reach upwards. The findings of this test established the spatial and temporal ability of animals (Nunez, 2008).

Y-maze test

Animals' short-term spatial memory was assessed using the Y-maze test as a means of recognizing. The apparatus constructed of plywood comprised of three arms. The length, height, and width of the arms were 50 cm, 32 cm, and 16 cm, respectively, and they crossed each other at an angle of 120°. After 1 h of the last dose, the rat was positioned near one of the arms and had the freedom to roam around the maze for about 10 min. Total count of entries using all four paws inside every arm were observed and noted properly. Spontaneous repetitions were determined as they manifested short-term memory and degree of arm entries without repetition, and this is also called alternation rate (Ghafouri *et al.*, 2016).

$$\text{Spontaneous alterations} = \text{Total number of arms entered} - 2 \quad (1)$$

$$\text{Alternation percentage} = \text{Actual alternation} \times 100 \quad (2)$$

Elevated maze test

This experiment was carried out to determine reminiscence, anxiety-like behavior as well as the learning ability of rodents. The maze designed for performance had four arms, each of 50 cm length and 10 cm breadth; two of the arms were open without walls, and remaining two were confined to 30-cm high walls. It was built of moderately dense board made up of fiber and has a dark surface. Each maze arm was hooked to robust plastic legs, elevating it 50 cm above the foundation (Walf and Frye, 2007). All the arms were visible to animals, and they were able to roam freely within them. On 38th day, after 60 min of drug administration, each animal was positioned at open arm of elevated maze. The time taken in each arm, total number, and movement from open into close arm were observed for 90 s. On 42nd day, after 24 h, the same practice was repeated to determine memory retention (Komada *et al.*, 2008).

Quantification of oxidative stress biomarkers

Levels of glutathione peroxidase (GPx), superoxide dismutase (SOD), lipid peroxidation, catalase, total protein contents, and reduced glutathione (GSH) were measured using brain homogenates.

Preparation of brain homogenate

Brain homogenate was prepared using 0.1-molar phosphate buffer with the help of a homogenizer. The homogenate had undergone centrifugation at 4000 rpm at a temperature of 4°C and the supernatant layer was separated, which was utilized for testing (Saleem *et al.*, 2022).

Measurement of malondialdehyde (MDA)

Approximately 3 mL of 0.38% thiobarbituric acid was added to 1 mL of aliquots of buoyant and stirred. After cooling in an ice bath, the mixture was centrifuged for 10 min at 3500 rpm and incubated of 15 min. The top layer was assessed by a 532-nm absorbance measurement (Ayaz *et al.*, 2022) by the following equation:

$$\text{Concentration of MDA} = \frac{\text{Abs} \times 100 \times \text{Vt}}{(1.56 \times 105) \times \text{weight of tissue} \times \text{Vu}}, \quad (3)$$

where:

Abs = absorption of sample at 532 nm;
Vt = complete volume of mixture;
Vu = aliquot volume.

Measurement of catalase activity

In order to measure the level of catalase, 0.05 mL of separated brain homogenate solution, 1.95 mL of 50-mM phosphate buffer, and 1-mL 30-mM hydrogen peroxide (H_2O_2) were combined to create a 3-mL mixture. Absorbance variations were noted at 240 nm. The coefficient of extinction of oxidized H_2O_2 in millimoles (mM) was calculated. The catalase activity (CAT) was measured in the form of μmol/min/mg of proteins (Fatima *et al.*, 2022) by the following equation:

$$\text{CAT} = \frac{\ddot{a}\text{O.D}}{\text{E} \times \text{Volume sample (mL)} \times \text{Protiens (mg)}} \quad (4)$$

where:

δO.D = minute changes in absorbance;
E = coefficient of extinction of H_2O_2 in mM.

Measurement of glutathione

Glutathione level was determined by mixing homogenized tissue (1 mL) with 10% trichloroacetic acid (TCA, 1 mL) prior to be used to assay GSH. In order to calculate absorbance at 412 nm, reagent 5,5′-dithiobis-(2-nitrobenzoic acid) (DTNB, 0.5 mL) was combined with

a fraction of supernatant and phosphate solution (4 mL) (Bais *et al.*, 2015):

$$GSH = \frac{y - 0.00314}{0.0314 \times \frac{Vf}{TxVU}}, \quad (5)$$

where:

Y = absorption of the sample;
D_F = diluting agent (1);
T = homogenate of tissue.
Vu = Quantity of the aliquot

Measurement of superoxide dismutase

A mixture of 1.2 mL of sodium phosphate buffer having 7.4 pH, 100-mL brain homogenate, 100-mL phenazine methosulfate (186 mM), about 200-mL triton X, 300 mL of nitro blue tetrazolium (300 mM) was formulated. The mixture was allowed to incubate at 30°**C** for about 95 s. The reaction process was halted by adding glacial acetic acid following the addition of 4 mL of n-butanol and settling it for about 10 min for isolation of n-butanol layer, which was centrifuged at 1000 rpm. Absorbance was recorded at 560 nm (Kim *et al.*, 2016).

Measurement of protein level

Two types of reagents were prepared to measure protein levels. Reagent 1 contained 1 mL of 0.5% copper sulfate and 2% sodium carbonate (Na_2CO_3; 48 mL) in 0.1-N NaOH. It also contained 1% sodium potassium tartrate (1 mL) in distilled water. This reagent was taken in a test tube along with brain homogenate and kept for about 10 min. The second reagent was prepared by taking 1 part of water and 2 parts of 0.5-mL folin phenol (2 N). Both reagents were mixed together and incubated for around 30 min at 37°C. The absorbance was recorded at 660 nm. The regression line was designed by taking different concentrations of bovine serum albumin (BSA) (Lowry et al, 1951).

Quantification of neurotransmitters

Aqueous phase formulation

A tissue specimen was prepared and centrifuged at 2000 rpm for 10 min with 5 mL of hydrochloric acid and butanol. After separating the upper layer, it was added to a sample tube along with 0.1-M HCL (0.31 mL) and heptane (2.5 mL). Following vigorous shaking, the mixture was left for 10 min and again centrifuged for 10 min at 2000 rpm. Two layers were formed: the upper one was decanted to test the level of neurotransmitters (Saleem *et al.*, 2022).

Measurement of serotonin level

Aqueous phase of 0.2 mL was mixed with 0.25 mL of o-phthaldialdehyde (OPT). Then for about 10 min, this mixture was heated to a temperature of 100°C and cooled to room temperature. Absorbance was determined at 440 nm (Saleem *et al.*, 2021).

Measurement of acetylcholinesterase

Acetylthiocholine iodide (20 µL), 2,4,dithiobis nitrobenzoic acid (100 µL), and phosphate buffer (2.6 mL; pH 8.00, 0.1 M) were combined. Brain homogenate (0.4 mL) was added to this mixture. The 2,4-dithiobisnitrobenzoic acid and thiocholine reaction developed a yellow color. At the end, absorbance was measured at 412 nm (Saleem *et al.*, 2020):

$$R = 5.74 \times 10^{-4} \times \frac{A}{CO}$$

where:

CO = actual quantity of tissues (mg/mL);
A = difference in absorbance per minute;
R = Speed of substrate hydrolysis per gram of tissue.

Measurement of noradrenaline and dopamine

Mixture of 0.4-M hydrochloric acid (0.05 mL), aqueous phase (0.2 mL), and sodium acetate buffer (0.1 mL) was formulated. Sodium sulphite (0.1 mL) was added to precede the process of oxidation. After about 90 s, 0.1-mL acetic acid and 100-µL Na_2SO_3 were added to the reaction mixture to stop oxidation process. This was then exposed to heating at 100°C for 5 min before cooling off. Then the absorption was measured at 359 nm and 450 nm (Saleem *et al.*, 2022).

Histopathological analysis of brain and vital organs

The rats were anesthetized with 10% isoflurane and slaughtered by cervical dislocation. Brain and all vital organs were removed and each organ was weighed accordingly. All vital organs were stored in 10% formalin solution, while the brain was retained in an ice-cold phosphate buffer (pH 7.4). The slides were prepared with hematoxylin and eosin (H&E) staining, and photographic images were captured at 40× resolution with the help of optical microscopic.

Statistical considerations

The numerical findings of the study were presented as mean ± standard error of mean (SEM). The results were statistically evaluated (by version 5 of Graph Pad Prism) by applying one-way ANOVA along with Bonferroni post-test and two-way ANOVA tailed by Tukey test; $p < 0.05$ was considered as statistically significant.

Results and Discussion

Behavioral observations

Open field test

The 2.5-, 5.0-, and 7.5-mg/kg CRBO-treated groups showed remarkable ($p < 0.001$) elevation in the physical activity of animals. The disease control group manifested a remarkable ($p < 0.001$) decrease in movement, compared to the control group (Figures 1–3).

Morris water maze test

On day 42, escape latency (EL) was measured for acquisition test. The disease control group displayed a substantial ($p < 0.001$) increase in comparison to the control group. Treatment groups with different doses of CRBO showed a remarkable ($p < 0.001$) fall in escape latency values, compared to the disease control group (Figure 4 and Table 1).

Y-maze test

The number of alterations, arm entries, and triads were measured. The disease control group manifested a remarkable ($p < 0.001$) drop in the entries compared to

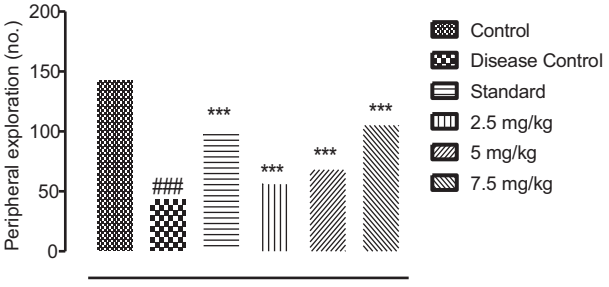

Figure 2. Effect of chamuangone-rich rice bran oil on experimental rats observing peripheral exploration in open field test. Mean ± SEM (n = 5) is applied to quantify the results. $^{\#}p < 0.05$, $^{\#\#}p < 0.01$, and $^{\#\#\#}p < 0.001$, compared to the control group. $^{*}p < 0.05$, $^{**}p < 0.01$, and $^{***}p < 0.001$, compared to the disease control group.

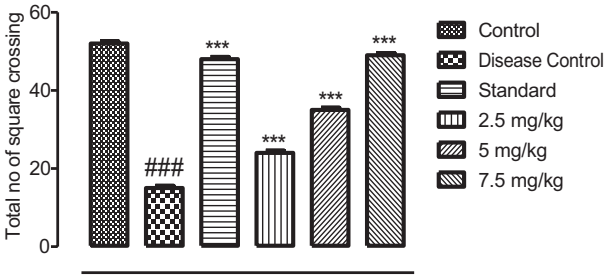

Figure 1. Effect of chamuangone-rich rice bran oil on experimental rats observing square crossing in open field test. Mean ± SEM (n = 5) is applied to quantify the results. $^{\#}p < 0.05$, $^{\#\#}p < 0.01$, and $^{\#\#\#}p < 0.001$ compared to the control group. $^{*}p < 0.05$, $^{**}p < 0.01$, and $^{***}p < 0.001$, compared to the disease control group.

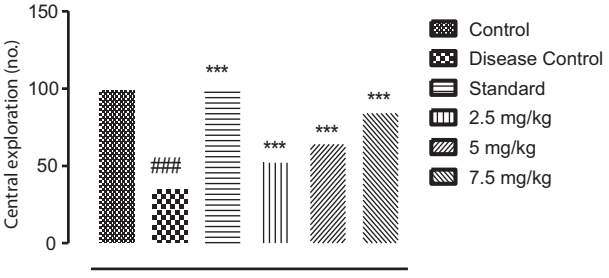

Figure 3. Effect of chamuangone-rich rice bran oil on experimental rats observing central exploration in open field test. Mean ± SEM (n = 5) is applied to quantify the results. $^{\#}p < 0.05$, $^{\#\#}p < 0.01$, and $^{\#\#\#}p < 0.001$, compared to the control group. $^{*}p < 0.05$, $^{**}p < 0.01$, $^{***}p < 0.001$, compared to the disease control group.

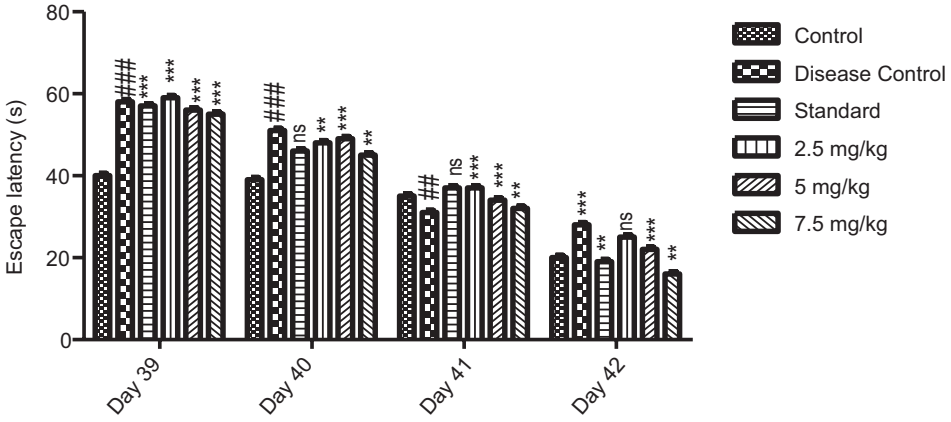

Figure 4. Effect of chamuangone-rich rice bran oil on escape latency in Morris water maze test. Mean ± SEM (n = 6) is applied to quantify the results. $^{\#}p < 0.05$, $^{\#\#}p < 0.01$, and $^{\#\#\#}p < 0.001$, compared to the control group. $^{*}p < 0.05$, $^{**}p < 0.01$, and $^{***}p < 0.001$, compared to the disease control group.

Table 1. Effect of chamuangone-rich rice bran oil on all quadrants of time latency in Morris's water maze test.

Groups	Dose (mg/kg)	North quadrant	South quadrant	East quadrant	West quadrant
Control		24.7 ± 0.57	13.6 ± 0.64	16.3 ± 0.52	17.3 ± 0.68
Disease control ($AlCl_3$ + D galactose)	150 + 150	42.0 ± 0.68###	37.0 ± 0.97###	38.5 ± 0.80###	52.5 ± 0.80###
Standard (rivastigmine)	3	22.5±0.69***	14.0 ± 0.57***	19.3 ± 0.69***	30.2 ± 0.58***
Treatment groups	2.5	40.3 ± 0.80*	35.0 ± 0.58***	37.0 ± 0.57	38.3 ± 0.58**
	5.0	31.4 ± 0.577***	29.0 ± 0.57***	40.0 ± 0.57*	33.0 ± 0.55***
	7.5	23.9 ± 0.06***	17.1 ± 0.55***	23.0 ± 0.80***	10.5 ± 0.58***

Mean ± SEM (n = 6) is applied to quantify the results. #$p < 0.05$, ##$p < 0.01$, ###$p < 0.001$, compared to the control group. *$p < 0.05$, **$p < 0.01$, ***$p < 0.001$, compared to the disease control group.

the control group. The dose-dependent CRBO treatment groups showed a remarkable ($p < 0.001$) dose-dependent improvement in alterations, triads, and entries (Figures 5–7).

Elevated maze test

On day 42 of the study, transfer latency was examined to ascertain animals' cognitive nature, which displayed a substantial ($p < 0.001$) increase in disease control, compared to the control group. Dose-dependent CRBO treatment groups showed a remarkable ($p < 0.001$) loss in transfer latency, compared to the standard group (Figure 8).

Biochemical Testing

The disease control group presented a substantial ($p < 0.001$) decrease in the levels of CAT, SOD, and GSH activity in comparison to the control group. The standard (rivastigmine) treatment group exhibited a remarkable ($p < 0.001$) elevation in these oxidative biomarkers, compared to the disease control group. Dose-dependent increase in the concentrations of CAT, SOD, and GSH were observed whereas the disease control

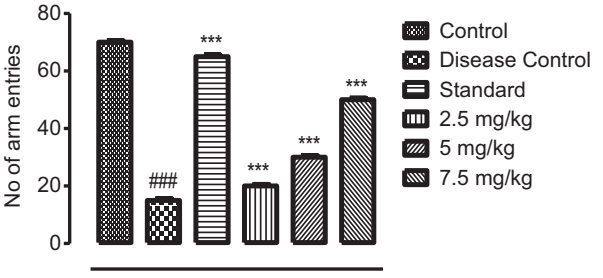

Figure 6. Effect of chamuangone-rich rice bran oil on experimental rats observing number of arm entries in Y-maze test. Mean ± SEM (n = 5) is applied to quantify the results. #$p < 0.05$, ##$p < 0.01$, and ###$p < 0.001$, compared to the control group. *$p < 0.05$, **$p < 0.01$, and ***$p < 0.001$, compared to the disease control group.

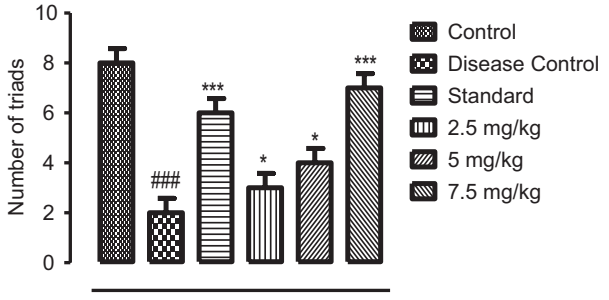

Figure 5. Effect of chamuangone-rich rice bran oil on experimental rats observing number of triads in Y-maze test. Mean ± SEM (n = 5) is applied to quantify the results. #$p < 0.05$, ##$p < 0.01$, and ###$p < 0.001$, compared to the control group. *$p < 0.05$, **$p < 0.01$, ***$p < 0.001$, compared to the disease control group.

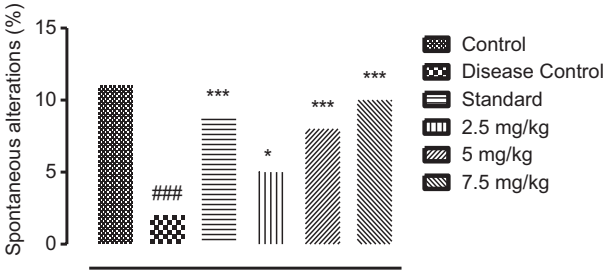

Figure 7. Effect of chamuangone-rich rice bran oil on experimental rats observing spontaneous alterations in Y-maze test. Mean ± SEM (n = 5) is applied to quantify the results. #$p < 0.05$, ##$p < 0.01$, and ###$p < 0.001$, compared to the control group. *$p < 0.05$, **$p < 0.01$, ***$p < 0.001$, compared to the disease control group.

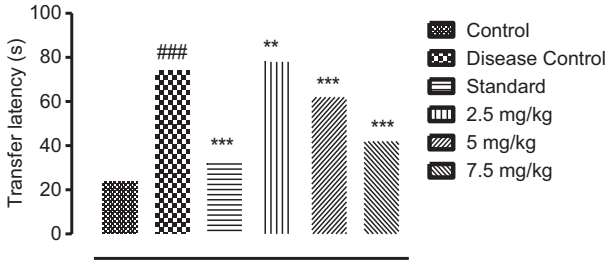

Figure 8. Effect of chamuangone-rich rice bran oil on experimental rats observing transfer latency in elevated maze test. Mean ± SEM (n = 5) is applied to quantify the results. $^{\#}p < 0.05$, $^{\#\#}p < 0.01$, and $^{\#\#}p < 0.001$, compared to the control group. $^{*}p < 0.05$, $^{**}p < 0.01$, and $^{***}p < 0.001$, compared to the disease control group.

group displayed a notable ($p < 0.001$) surge in MDA level, compared to the control group, and after the administration of CRBO, the concentration of MDA decreased in a dose-dependent manner (Table 2).

Quantification of Neurotransmitters

Measurement of acetylcholinesterase

Acetylcholinesterase was remarkably ($p < 0.001$) elevated in the disease control group in comparison to the control group. Significant ($p < 0.001$) decrease in enzyme levels was observed, being the lowest at 7.5 mg/kg of CRBO as compared to 2.5, 5.0 mg/kg and the standard (Figure 9).

Measurement of serotonin, dopamine, and noradrenaline

Levels of serotonin, dopamine, and noradrenaline declined remarkably ($p < 0.001$) in the disease control group, compared to the control group. CRBO-treated mice displayed a significant ($p < 0.001$) increase at 2.5, 5.0, and 7.5 mg/kg in the levels of these neurotransmitters as compared to the disease control group (Tables 3–5).

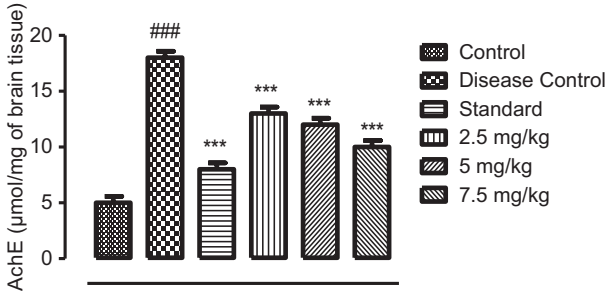

Figure 9. Effect of chamuangone-rich rice bran oil on brain AchE activity. Mean ± SEM (n = 6) is applied to quantify the results. $^{\#}p < 0.05$, $^{\#\#}p < 0.01$, and $^{\#\#\#}p < 0.001$, compared to the control group. $^{*}p < 0.05$, $^{**}p < 0.01$, and $^{***}p < 0.001$, compared to the disease control group.

Table 2. Effect of chamuangone-rich rice bran oil on biochemical markers in brain homogenate.

Groups	Dose (mg/kg)	Catalase (mmol/mg)	Superoxide dismutase (µg/mg of proteins)	Malondialdehyde (µmol/mg of proteins)	Reduced glutathione (µg/mg of proteins)	Glutathione peroxidase (µg/mg of proteins)
Control	--	3.8 ± 0.06	1.4 ± 0.02	5.9 ± 0.06	0.8 ± 0.02	7.9 ± 0.03
Disease control ($AlCl_3$ + D galactose)	150 + 150	2.1 ± 0.06$^{\#\#\#}$	0.9 ± 0.01$^{\#\#\#}$	7.8 ± 0.04$^{\#\#\#}$	0.2 ± 0.01$^{\#\#\#}$	5.6 ± 0.01$^{\#\#\#}$
Standard (rivastigmine)	3	3.4 ± 0.11***	1.3 ± 0.06***	6.0 ± 0.02***	0.9 ± 0.03***	8.3 ± 0.02**
Treatment groups	2.5	3.1 ± 0.01***	1.1 ± 0.01***	6.2 ± 0.01***	0.7 ± 0.02***	8.6 ± 0.04**
	5	3.3 ± 0.02***	1.2 ± 0.04***	6.1 ± 0.21***	0.4 ± 0.05***	8.4 ± 0.01**
	7.5	3.5 ± 0.06***	1.5 ± 0.01***	5.8 ± 0.06***	0.3± 0.02*	9.1 ± 0.06***

Mean ± SEM (n = 6) is applied to quantify the results. $^{\#}p < 0.05$, $^{\#\#}p < 0.01$, and $^{\#\#\#}p < 0.001$ differed from the control group. $^{*}p < 0.05$, $^{**}p < 0.01$, and $^{***}p < 0.001$ differed from the disease control group.
SOD: superoxide dismutase; CAT: catalase activity; MDA: malondialdehyde; GSH: glutathione; GPx: glutathione peroxidase.

Table 3. Measurement of serotonin levels in brain homogenate.

Groups	Dose (mg/kg)	Serotonin (µg/mg)
Control	–	0.90 ± 0.006
Disease control ($AlCl_3$ + D-galactose)	150 + 150	0.30 ± 0.04###
Standard (rivastigmine)	3	0.87 ± 0.006***
Treatment groups	2.5	0.62 ± 0.11***
	5.0	0.68 ± 0.006***
	7.5	0.72 ± 0.02***

Mean ± SEM (n = 6) is applied to quantify the results. #$p < 0.05$, ##$p < 0.01$, and ###$p < 0.001$ differed from the control group. *$p < 0.05$, **$p < 0.01$, and ***$p < 0.001$ differed from the disease control group.

Table 4. Measurement of dopamine levels in brain homogenate.

Groups	Dose (mg/kg)	Dopamine (µg/mg)
Control	–	0.7 ± 0.006
Disease control ($AlCl_3$ + D-galactose)	150 + 150	0.3 ± 0.11###
Standard (rivastigmine)	3	0.7 ± 0.01***
Treatment groups	2.5	0.3 ± 0.04***
Control	5.0	0.4 ± 0.21***
Disease control ($AlCl_3$ + D-galactose)	7.5	0.5 ± 0.03***

Mean ± SEM (n = 6) is applied to quantify the results. #$p < 0.05$, ##$p < 0.01$, and ###$p < 0.001$ differed from the control group. *$p < 0.05$, **$p < 0.01$, and ***$p < 0.001$ differed from the disease control group.

Table 5. Measurement of noradrenaline levels in brain homogenate.

Groups	Dose (mg/kg)	Noradrenaline (µg/mg)
Control		0.7 ± 0.05
Disease control ($AlCl_3$ + D-galactose)	150 + 150	0.3 ± 0.04###
Standard (rivastigmine)	3	0.7 ± 0.05***
Treatment groups	2.5	0.3 ± 0.06**
	5.0	0.4 ± 0.01*
	7.5	0.5 ± 0.03***

Mean ± SEM (n = 6) is applied to quantify the results. #$p < 0.05$, ##$p < 0.01$, and ###$p < 0.001$ differed from the control group. *$p < 0.05$, **$p < 0.01$, and ***$p < 0.001$ differed from the disease control group.

Measurement of protein level

There was a remarkable decrease ($p < 0.001$) in protein levels in the disease control group, compared to the control group. Substantial ($p < 0.001$) elevation in protein levels were discovered when treated with dose-dependent CRBO. Mean value at a dose of 7.5-mg/kg CRBO was 69 ± 0.57 whereas the standard dose showed a mean value of 60 ± 0.68, both values showed mutual resemblance (Table 6).

Table 6. Measurement of protien levels in brain homogenate.

Groups	Dose (mg/kg)	Protein (µg/mg)
Control		90.0 ± 0.57
Disease control ($AlCl_3$ + D-galactose)	150 + 150	44.0 ± 0.57###
Standard (rivastigmine)	3	60.0 ± 0.68***
Treatment groups	2.5	50.0 ± 0.57***
	5.0	67.0 ± 0.68***
	7.5	69.0 ± 0.57***

Mean ± SEM (n = 6) is applied to quantify the results. #$p < 0.05$, ##$p < 0.01$, and ###$p < 0.001$ differed from the control group. *$p < 0.05$, **$p < 0.01$, and ***$p < 0.001$ differed from the disease control group.

Examination of histopathology of brain and vital organs

Histopathological examination of brain

The control group had normal brain tissue patterns; on the other hand, the disease control group had evidences of neurodegeneration, such as necrosis, origination of plaques, NFTs, and loss of neurons along with vacuolization. CRBO-treated groups showed dose-dependent restoration in neuronal cells and recovery of NFTs, senile plaques, and vacuolization. The standard group showed resemblance to the control group (Figure 10).

Histopathological analysis of vital organs

Treatment with CRBO did not produce any noticeable toxicity to vital organs. The histology of heart tissues displayed normal myocardial fibers in the groups treated with CRBO, resembling normal heart tissues of the control group. Nevertheless, minor vascular congestion was observed in the disease control group animals, differed from the control group (Figure 11). The disease control group revealed congestion in the renal parenchyma and nuclei whereas CRBO treatment did not cause any abnormality in renal tissues (Figure 12). Figure 13 shows that liver cells (hepatocytes) contained sinusoids that formed a linkage starting from the hepatic artery, reaching the central portal vein. In CRBO-treated groups, normal hepatocytes were observed, resembling the control group without any fibrosis. In the disease control group, the hepatocytes exhibited congestion, vacuolization, and fibrosis, compared to the control group. In both control and standard groups, lung tissues displayed normal epithelium, bronchioles, and pulmonary alveoli. Treatment

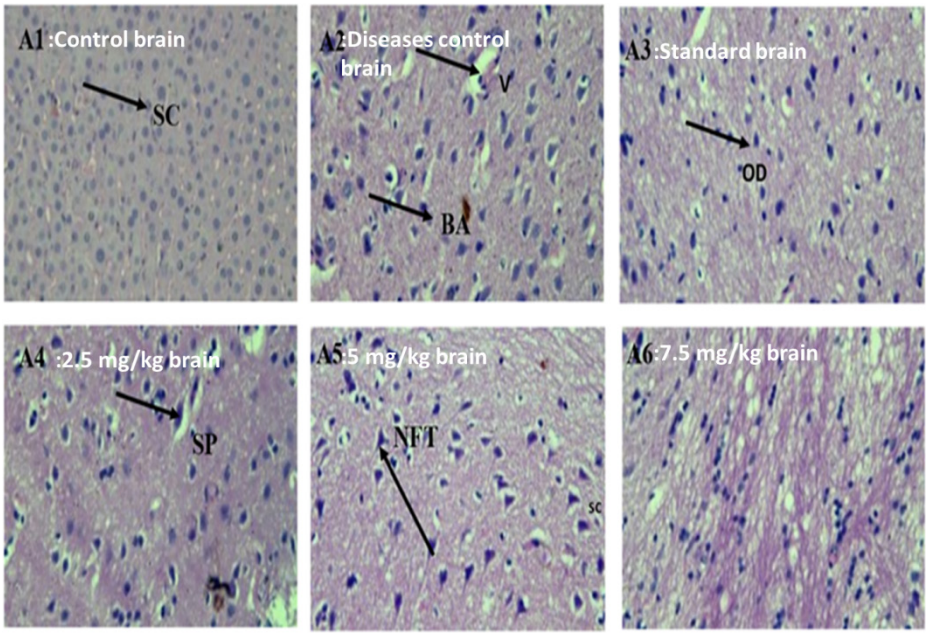

Figure 10. Effect of chamuangone-rich rice bran oil on the brain histology of mice. A: brain, 1: control; 2: disease control; 3: standard; 4: 2.5 mg/kg; 5: 5.0 mg/kg; 6: 7.5 mg/kg. SC: satellite cells; SP: senile plaques; V: vacuolization; BA: beta amyloid; OD: oligodenrites; NFTs: neurofibrillary tangles.

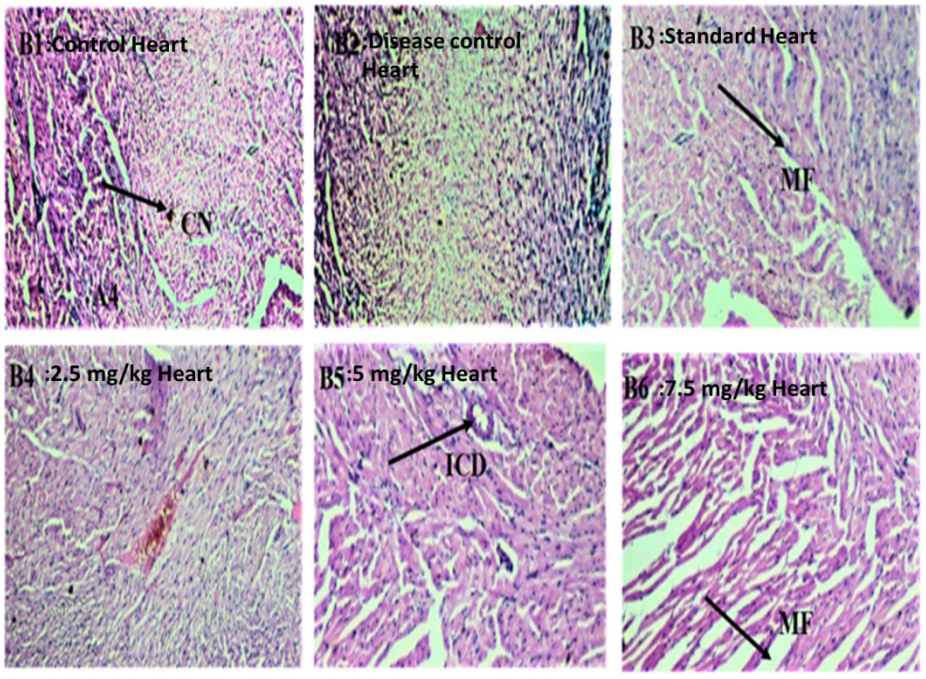

Figure 11. Effect of chamuangone-rich rice bran oil on the heart histology of mice. 1: control; 2: disease control; 3: standard; 4: 2.5 mg/kg; 4: 5.0 mg/kg; 6: 7.5 mg/kg. B: heart; CN: central nuclei; MF: myocardial fibrils; ICD: intercalated discs.

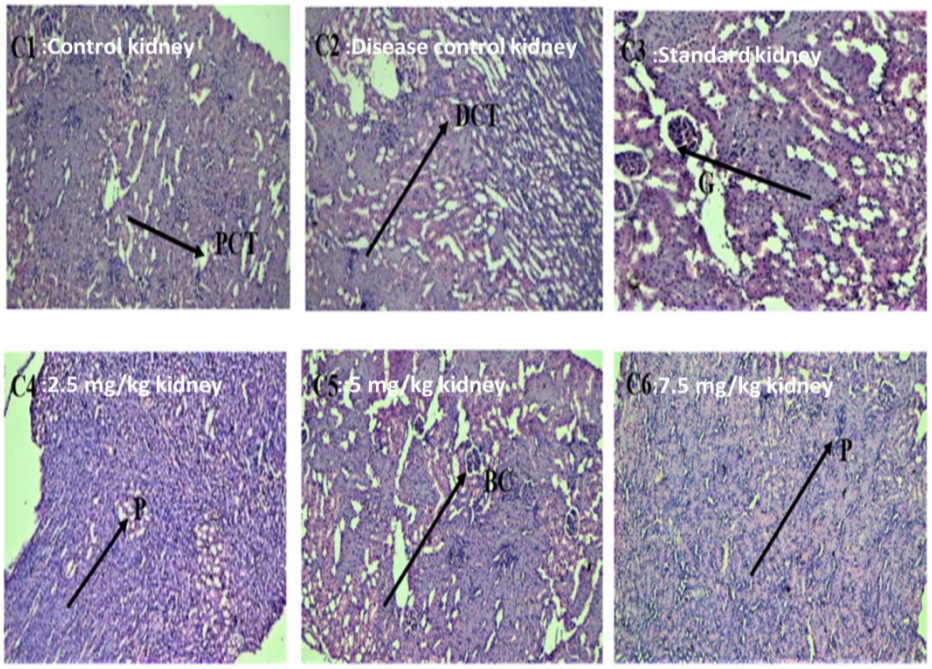

Figure 12. Effect of chamuangone-rich rice bran oil on the kidney histology of mice. 1: control; 2: disease control; 3: standard; 4: 2.5 mg/kg; 5: 5.0 mg/kg; 6: 7.5 mg/kg. C: kidney; PCT: proximal convoluted tubule; DCT: distal convoluted tubule; G: glomerulus; P: podocytes; BC: Bowman's capsule.

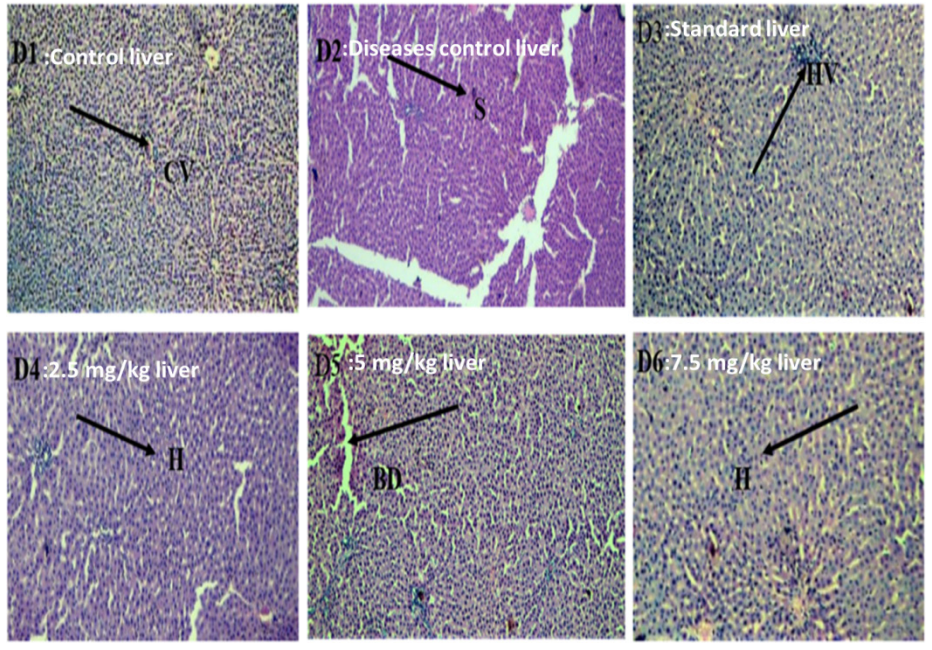

Figure 13. Effect of chamuangone-rich rice bran oil on the liver histology of mice. 1: control; 2: disease control; 3: standard; 4: 2.5 mg/kg; 5: 5.0 mg/kg; 6: 7.5 mg/kg. D: liver; CV: central vein; S: sinusoid; HV: hepatic vein; H: hepatocytes; BD: bile duct.

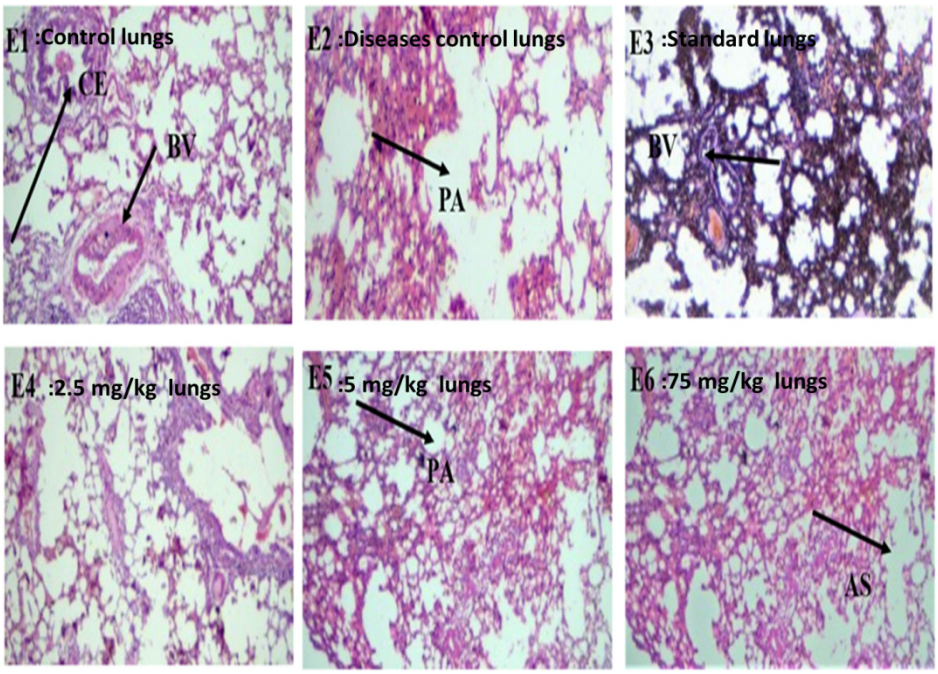

Figure 14. Effect of chamuangone-rich rice bran oil on the lung histology of mice. 1: control; 2: disease control; 3: standard; 4: 2.5 mg/kg; 5: 5.0 mg/kg; 6: 7.5 mg/kg. E: lungs; CE: columnar epithelium; BV: blood vessels; PA: pulmonary alveoli; AS: alveolar sac.

with CRBO did not produce abnormal changes in lung tissues whereas the disease control showed moderate level of congestion (Figure 14).

Discussion

Progressive degeneration of certain vulnerable groups of neurons is a characteristic of neurodegenerative disorders such as AD (Dugger and Dickson, 2017). AD is a brain disease caused by neurodegenerative conditions, such as changes in cognition, behavior, and function (Cerquera-Jaramillo *et al.*, 2018). Preclinical AD affects almost eight times more people, compared to symptomatic AD, eventually putting them at a risk of the illness (Cummings *et al.*, 2018). Age and genetics are the risk factors that cannot be avoided. The most defining aspect of AD is memory impairment, which first affects recent episodic memory with progression of the disease. Atypical cases, however, may appear with no amnestic ailment, such as predominance of language, visuospatial working memory, or executive function abnormalities, which commonly affect individuals aged <65 years (Ulep *et al.*, 2018).

The World Health Assembly (WHA), the decision-making body of World Health Organization (WHO), has adopted global strategy for society's health response to AD; it calls for increased recognition, exploration, and new techniques to address this critical medical problem (Javaid *et al.*, 2021). Over 122,000 individuals died from AD in 2018, a 146% increase from 2000.

Alzheimer's disease is very expensive for the society, with significant costs associated with medical treatment and caretaking (Piovesan *et al.*, 2023). The clinical manifestations of AD are somewhat alleviated by AchE inhibitors and NMDA antagonists; however, currently no medication is available with a substantial disease-altering effects (Citron, 2004). Clinical trials of combined AD treatments are in progress, focusing on four primary domains: neurodegeneration, cognitive dysfunction, alleged neuroregeneration, and manifestations that are not related to cognition. Targeting of noncognitive manifestations in AD patients is practiced using both herbal and pharmacological therapies (Nagata *et al.*, 2022).

Investigation of AD has resulted in the identification of numerous targets, including all types of histamines, serotonin, cholinergic, monoamine oxidase inhibitors, glycogen synthase kinase-3 (GSK-3), and N-methyl-D-aspartate receptors (NMDAR) that affect the development and aggravation of the illness. Based on these targets, many potent and efficacious therapies for the treatment of AD have been discovered. However, only donepezil, galantamine, rivastigmine, and memantine have received the FDA approval for AD treatment. They are all single-target drugs that may significantly boost

patients' loss of memory and cognitive decline, but they cannot completely reverse the condition (Yiannopoulou and Papageorgiou, 2020).

Reactive oxygen species (ROS) produced within cells cause neurodegeneration, which is featured by malfunctioning or neuronal death. Acute brain injury is also a common cause. Cysteine/glutamate antiporter system performs poorly if excessive amount of glutamate is present, with production of ROS and depletion of glutathione levels. A cellular oxidative stress causes the mitochondria to fail and opens door for caspase independent apoptosis pathway (Nguyen *et al.*, 2022).

Dementia may be prevented by other ways than using drugs, such as nutritional therapy and lifestyle changes, that are effective in a number of metabolic diseases associated with aging, such diabetes, cardiovascular disease (CVD), obesity, and cancer. These non-pharmacological therapies could be helpful at slowing down AD and in reducing the financial load on both patients and caretakers (Bhatti *et al.*, 2020).

Isolated from the leaves of *Garcinia cowa*, chamuangone contains active constituents that exhibit various pharmacological activities. Literature showed that extraction of chamuangone was carried out by utilizing n-Hexane; however, alternative green solvents, such as vegetable oils (e.g. rice bran oil), are used to obtain higher yield (Sae-Lim *et al.*, 2019a). Isolated chemicals and extracts derived from different portions of *G. cowa* have revealed interesting bioactivities, such as antioxidant, cytotoxic, antibacterial, antimalarial, anti-inflammatory, and antimicrobial properties.

Mice were used to create a 42-day AD model by subcutaneously delivering D-galactose to animals to trigger the disease and to study the possible anti-AD properties of CRBO. One of the main neurotoxins, aluminium chloride, causes buildup in brain mitochondrial malfunctioning and dramatically accelerates the mutation of DNA and proteins and ROS. The fundamental cause of AD, which destroys neurons by escalating oxidative stress, is the extended and substantial exposure to aluminium (chloride) toxicity. This oxidative pressure modified cellular working, subdued antioxidant defense system, and produced structural defect to functional proteins that led to AD (Yin *et al.*, 2020).

Low-dose D-galactose intervention over an extended period of time led to abnormalities that resembled natural aging processes in animals, including oxidative stress, cognitive impairment, a weakened immune system, and changes in gene transcription. Mice exposed to D-galactose over an extended period also developed neurotoxicity, and was utilized as a model to examine the mechanism of AD. Aluminum and d-galactose imitating cognitive deficits and diseases similar to AD served as useful models for researching AD treatments (Mahdi *et al.*, 2021). With the modification of behavioral and biochemical indicators, in the current study, aluminum chloride- and D-galactose-induced memory impairment was alleviated by CRBO (Kamel *et al.*, 2018). By interacting with the central nervous system's (CNS) AchE enzyme, aluminum chloride and D-galactose led to ongoing stress that impaired cognition (Xing *et al.*, 2018). Because of the extra release of ROS, the body was unable to eliminate it, resulting in oxidative stress. Biochemical studies were conducted to assess endogenous antioxidant capacity (Mantzavinos and Alexiou, 2017). By regulating both motor and non-motor dysfunctions, CRBO and rivastigmine were compared in this study. The behavioral and physiological alterations brought on by aluminium chloride and D-galactose were lessened by CRBO (Saleem *et al.*, 2022). CRBO restored both behavioral and metabolic alterations in AD model.

The current study explained the neuroprotective effects of CRBO, as administration of aluminum chloride and D-galactose caused cognitive behavioral alteration coupled with locomotor impairments (Singh *et al.*, 2018). To evaluate locomotor and exploratory activities, the open field test entailed exploring both center and periphery squares. While the disease control group showed reduced exploration, all CRBO-treated groups and rivastigmine-treated group showed improvement in square crossing (Ahmadi *et al.*, 2017). Evaluation of hippocampus-dependent memory and spatial learning was caused using the Morris water maze test (Sharma *et al.*, 2019). Animals' persistent cognition and capacity to use alternative arms was measured by using the Y-maze test; these were decreased in mice receiving chronic AD induction agents (Lu *et al.*, 2020). The transfer latency of elevated maze test was decreased in retention phase on day 42 in the animals of acquisition trial conducted on day 41. CRBO treatment groups displayed decreased transfer latency compared to the disease control animals and showed effects that lessened dementia as well as cognition (Pairojana *et al.*, 2021). The results showed that CRBO and rivastigmine reduced memory and retention impairments generated by aluminum chloride and D-galactose.

Lipid peroxidation is an intricate procedure connecting the conjugation of oxidative radicals with polyunsaturated fats, producing a range of extremely reactive conductive aldehydes (Reed, 2011). One of the primary targets of the lipid peroxidation process is the CNS (Sultana *et al.*, 2013). AD patients have increased polyunsaturated fatty acid (PUFA) oxidation, impaired antioxidant defense, more oxygen intake, and oxidative stress in their cortex with regional variations in the mitochondria (Ansari and Scheff, 2010). A strong correlation between

free-radical-induced injury and the disease's neuropathology is demonstrated by assessing the activity of antioxidant enzymes and their co-localization to senile plaques and dystrophic neurites. It has been demonstrated that a lack of GSH may contribute to a variety of human disorders (Zhang *et al.*, 2023). GSH levels showed a decrease in AD groups but increase in treatment groups.

Catalase is a crucial enzyme and uncharged of eliminating hydrogen peroxide by its breakdown hence preserving the optimum amount of the compound in the cell, which is for normal signaling activities. Catalase deficiency has been linked to many age-related degenerative disorders, including AD (Nandi *et al.*, 2019). The catalase level was evaluated via the superior and middle temporal gyri, as well as AD hippocampus, which showed elevation compared to the disease control group (Lovell *et al.*, 1995; Padurariu *et al.*, 2010). All cells produce ROS from biochemical and molecular pathways, such as superoxide and hydrogen peroxide. These ROS have potential to disrupt oxidatively membrane lipids, proteins, and DNA if their levels are not regulated. An internal antioxidant enzyme called glutathione peroxidase-1 (GPx-1) converts hydrogen peroxide enzymatically to water to mitigate its adverse effects. Thus, GPx-1 controls these processes by reducing the buildup of hydrogen peroxide (Lubos *et al.*, 2011).

Superoxide dismutase is a unique anti-oxidant enzyme that eliminates anion superoxide by converting it to hydrogen and oxygen peroxide, preventing the formation of peroxynitrite (a reactive oxidant), which causes additional damage (Rudan *et al.*, 2015). Multiple AD characteristics have been linked to decreased levels of SOD, such as acceleration of plaque deposition and increased tau phosphorylation. Memory impairment and buildup of amyloid plaque are two pathogenic processes in AD that are significantly lowered by mitochondrial superoxide. Both GPx and SOD catalyses eliminate hydrogen peroxide, which produces harmful hydroxyl radicals. CRBO showed a remarkable increase in GPx and SOD levels in a dose-dependent manner.

Another indicator of oxidative damage is MDA which interacts with functional groups of protein molecules, lipoproteins, DNA, and RNA because it is a highly reactive dialdehyde generated following the decomposition of peroxidized PUFAs. MDA is potentially dangerous because it can cross-link proteins and induce mutagenesis. It was previously linked in the development of various neurodegenerative illnesses, aging, diabetes mellitus, and brain ischemia (Landau *et al.*, 2013). The levels of MDA were higher in the disease control group and low in the treatment groups. Assessment of MDA levels is a very widely used method for determining lipid peroxidation decree that helps assess the stage of AD (Casado *et al.*, 2008).

Neurotransmitters, such as dopamine, noradrenaline, and serotonin, showed marked elevation in treatment groups whereas the disease control groups exhibited a decline in the levels of these neurotransmitters. AchE, a neurotransmitter, is revealed by parasympathetic neurons, plays a role in transducing signals that have an impact on recalling and learning. Cholinergic neurons are widely distributed in human brain. AchE affects neural systems like the amygdala, striatum, and hippocampus and is essential for memory improvement. AChE signaling is essential for cognitive functioning and control of inflammation. AD patients frequently exhibit AChE depletion and cholinergic signal transduction damage (Chen *et al.*, 2022). Because oxidative stress impairs adenosine triphosphate (ATP) and acetyl formation, which in turn increases cholinesterase activity and decreases AchE activity in the hippocampus, animals given D-galactose may experience cholinergic deficits. The disease control group receiving aluminum chloride and D-galactose demonstrated a noticeably elevated level of AchE. CRBO- and rivastigmine-treated animals, however, displayed a subsequent drop in AchE levels, supporting the anti-Alzheimer's activity of CRBO (Saleem *et al.*, 2022). Examination of brain tissue samples using histopathology revealed that treatment with CRBO significantly improved the formation of NFTs, vacuolization, and senile plaques in the brain, which are hallmark features of AD. However, the disease control group showed no significant changes in the histology of vital organs, except for some degree of vascular congestion in the heart, parenchymal congestion in the kidney, and hepatic fibrosis. However, treatment with CRBO reversed these changes, indicating a potential therapeutic effect on AD-related pathology.

Conclusions

The conclusion demonstrates a complete assortment of biochemical analysis—reduced AchE activity, increased GSH levels, and heightened CAT. Free radical-eliminating and anti-inflammatory activities of CRBO demonstrate its neuroprotective impact in D-galactose- and aluminum chloride-induced AD neuroinflammation and memory impairment. These results underscore the nanocarriers' ability to modulate neurotransmitter levels and counteract oxidative stress, reaffirming their potential as a promising therapeutic tool. Furthermore, our histological analysis of hippocampal regions reinforces the protective properties of CRBO. This protective effect is notably conspicuous when compared to the disease control group, showcasing the preservation of neuronal integrity, a reduction in dark neurons, and a decrease in

pathological features within the treated groups. These findings highlight the substantial promise of CRBO in safeguarding brain health and mitigating neurodegenerative processes. The findings offer novel information that highlights CRBO as a viable therapy for diseases with neurodegenerative etiologies. However, further investigation is required to clarify the precise molecular foundation of AD treatment.

Author Contributions

Uzma Saleem, Muhammad Ajmal Shah, Pharkphoom Panichayupakaranant, and Ana Sanches Silva conceived and designed the research. Badriyah S. Alotaibi, Sadaf Waseem, Zunera Chaudhary, and Maryam Farrukh performed the experiments. Ifat Alsharif, Wedad Saeed Alqahtani, Abdullah R. Alanzi, Mona N. BinMowyna, Yasmene F. Alanazi, Abdulelah M. Almuwallad, Abdulmajid M. Almuwallad, and Khairul Anam analyzed and interpreted the data. All authors contributed equally to the preparation, revision, and final approval of the manuscript for submission.

Conflicts of Interest

The authors declared no conflict of interest.

Data Availability Statement

Original contributions presented in the study are included in the article. Further inquiries can be directed to the corresponding authors.

Acknowledgments

Authors gratefully acknowledge the Princess Nourah bint Abdulrahman University Researchers Supporting Project number (PNURSP2024R73), Princess Nourah bint Abdulrahman University, Riyadh, Saudi Arabia. Authors extend their appreciation to researchers supporting project number (RSPD2024R885) at King Saud University Riyadh Saudi Arabia for supporting this research. Thanks to Universitas Diponegoro, Indonesia, through Adjunct Professor, World-Class University Program 2024. Ana Sanches Silva thanks FCT/MCTES for funding (UIDB/00211/2020).

References

Ahmadi, M., Rajaei, Z., Hadjzadeh, M., Nemati, H. and Hosseini, M. 2017. Crocin improves spatial learning and memory deficits in the Morris water maze via attenuating cortical oxidative damage in diabetic rats. Neurosci Lett. 642:1–6. https://doi.org/10.1016/j.neulet.2017.01.049

Alotaibi, B.S., Saleem, U., Ahmad, A., Chaudhary, Z., Farrukh, M., Khayat R.O., et al. 2024. Chamuangone-enriched rice bran oil ameliorates neurodegeneration in haloperidol-induced Parkinsonian rat model via modulation of neuro-inflammatory mediators and suppression of oxidative stress markers. Italian J Food Sci., 36(2):163–180. https://doi.org/10.15586/ijfs.v36i2.2551

Ansari, M.A. and Scheff, S.W. 2010. Oxidative stress in the progression of Alzheimer's disease in the frontal cortex. J Neuropathol Exp Neurol. 69(2):155–167. https://doi.org/10.1097/NEN.0b013e3181cb5af4

Ayaz, M., Anwar, F., Saleem, U., Shahzadi, I., Ahmad, B., Mir, A. and Ismail, T. 2022. Parkinsonism attenuation by antihistamines via downregulating the oxidative stress, histamine, and inflammation. ACS Omega. 7(17):14772–14783. https://doi.org/10.1021/acsomega.2c00145

Bais, S., Gill, N. and Kumar, N. 2015. Neuroprotective effect of Juniperus communis on chlorpromazine-induced Parkinson's disease in animal model. Chinese Journal of Biology, 2015:1–7. https://doi.org/10.1155/2015/542542

Bhatti, G.K., Reddy, A.P., Reddy, P.H. and Bhatti, J.S. 2020. Lifestyle modifications and nutritional interventions in aging-associated cognitive decline and Alzheimer's disease. Front Aging Neurosci. 11:369. https://doi.org/10.3389/fnagi.2019.00369

Caraci, F., Santagati, M., Caruso, G., Cannavò, D., Leggio, G. M., Salomone, S., et al. 2020. New antipsychotic drugs for the treatment of agitation and psychosis in Alzheimer's disease: focus on brexpiprazole and pimavanserin. F1000Res. 9:F1000 Faculty Rev-686. https://doi.org/10.12688/f1000research.22662.1

Casado, A., Encarnación López-Fernández, M., Concepción Casado, M. and de La Torre, R. 2008. Lipid peroxidation and antioxidant enzyme activities in vascular and Alzheimer's dementias. Neurochem Res. 33:450–458. https://doi.org/10.1007/s11064-007-9453-3

Cerquera-Jaramillo, M.A., Nava-Mesa, M.O., González-Reyes, R.E., Tellez-Conti, C. and de-la-Torre, A. 2018. Visual features in Alzheimer's disease: from basic mechanisms to clinical overview. Neural Plasticity. 2018:1–21. https://doi.org/10.1155/2018/2941783

Chauhdary, Z., Saleem, U., Ahmad, B., Shah, S. and Shah, M.A. 2019. Neuroprotective evaluation of Tribulus terrestris L. in aluminum chloride induced Alzheimer's disease. Pak J Pharm Sci. 32(Sppl.2):805–816.

Chen, Z.-R., Huang, J.-B., Yang, S.-L. and Hong, F.-F. 2022. Role of cholinergic signaling in Alzheimer's disease. Molecules. 27(6):1816. https://doi.org/10.3390/molecules27061816

Chen, Z. and Zhong, C. 2014. Oxidative stress in Alzheimer's disease. Neurosci Bullet. 30:271–281. https://doi.org/10.1007/s12264-013-1423-y

Citron, M. 2004. Strategies for disease modification in Alzheimer's disease. Nature Rev Neurosci. 5(9):677–685. https://doi.org/10.1038/nrn1495

Craig-Schapiro, R., Fagan, A.M. and Holtzman, D.M. 2009. Biomarkers of Alzheimer's disease. Neurobiol. Dis. 35(2):128–140. https://doi.org/10.1016/j.nbd.2008.10.003

Cummings, J., Lee, G., Ritter, A. and Zhong, K. 2018. Alzheimer's disease drug development pipeline: 2018. Alzheimers Dement (NY). 4:195–214. https://doi.org/10.1016/j.trci.2018.03.009

Dugger, B.N. and Dickson, D.W. 2017. Pathology of neurodegenerative diseases. Cold Spring Harbor Perspect Biol. 9(7):a028035. https://doi.org/10.1101/cshperspect.a028035

Fatima, N., Anwar, F., Saleem, U., Khan, A., Ahmad, B., Shahzadi, I. et al. 2022. Antidiabetic effects of Brugmansia aurea leaf extract by modulating the glucose levels, insulin resistance, and oxidative stress mechanism. Front Nutr. 9:1005341. https://doi.org/10.3389/fnut.2022.1005341

Förstl, H. and Kurz, A. 1999. Clinical features of Alzheimer's disease. Eur Arch Psychiatry Clin Neurosci. 249:288–290. https://doi.org/10.1007/s004060050101

Ghafouri, S., Fathollahi, Y., Javan, M., Shojaei, A., Asgari, A. and Mirnajafi-Zadeh, J. 2016. Effect of low frequency stimulation on impaired spontaneous alternation behavior of kindled rats in Y-maze test. Epilepsy Res. 126:37–44. https://doi.org/10.1016/j.eplepsyres.2016.06.010

Hampel, H., Mesulam, M.-M., Cuello, A.C., Farlow, M.R., Giacobini, E., Grossberg, G.T., et al. 2018. The cholinergic system in the pathophysiology and treatment of Alzheimer's disease. Brain. 141(7):1917–1933. https://doi.org/10.1093/brain/awy132

Hua, X., Lei, M., Zhang, Y., Ding, J., Han, Q., Hu, G., et al. 2007. Long-term D-galactose injection combined with ovariectomy serves as a new rodent model for Alzheimer's disease. Life Sci. 80(20):1897–1905. https://doi.org/10.1016/j.lfs.2007.02.030

Jadhav, R.P., Kengar, M.D., Narule, O.V., Koli, V.W. and Kumbhar, S.B. 2019. A review on Alzheimer's Disease (AD) and its herbal treatment of Alzheimer's Disease. Asian J Res Pharm Sci. 9(2):112–122. https://doi.org/10.5958/2231-5659.2019.00017.1

Javaid, S.F., Giebel, C., Khan, M.A. and Hashim, M.J. 2021. Epidemiology of Alzheimer's disease and other dementias: rising global burden and forecasted trends. F1000Res. 10:425. https://doi.org/10.12688/f1000research.50786.1

Kamel, A.S., Abdelkader, N.F., Abd El-Rahman, S.S., Emara, M., Zaki, H.F. and Khattab, M.M. 2018. Stimulation of ACE2/ANG (1–7)/Mas axis by diminazene ameliorates Alzheimer's disease in the D-galactose-ovariectomized rat model: role of PI3K/Akt pathway. Mol Neurobiol. 55:8188–8202. https://doi.org/10.1007/s12035-018-0966-3

Kim, J.-B., Kopalli, S.R. and Koppula, S. 2016. Cuminum cyminum Linn (Apiaceae) extract attenuates MPTP-induced oxidative stress and behavioral impairments in mouse model of Parkinson's disease. Trop J Pharm Res. 15(4):765–772. https://doi.org/10.4314/tjpr.v15i4.14

Kim, D. and Tsai, L.-H. 2009. Bridging physiology and pathology in AD. Cell. 137(6):997–1000. https://doi.org/10.1016/j.cell.2009.05.042

Komada, M., Takao, K. and Miyakawa, T. 2008. Elevated plus maze for mice. JoVE. 22. https://doi.org/10.3791/1088-v

Kumar, A. and Singh, A. 2015. A review on Alzheimer's disease pathophysiology and its management: an update. Pharmacol Rep. 67(2):195–203. https://doi.org/10.1016/j.pharep.2014.09.004

Landau, G., Kodali, V.K., Malhotra, J.D. and Kaufman, R.J. 2013. Detection of oxidative damage in response to protein misfolding in the endoplasmic reticulum. In: Cadenas, E. and Packer, L. (Eds.) Methods in enzymology, Chap. 14, Vol. 526, pp. 231–250. Academic Press, Cambridge, MA. https://doi.org/10.1016/B978-0-12-405883-5.00014-4

Lopez, O.L., Becker, J.T., Sweet, R.A., Klunk, W., Kaufer, D. I., Saxton, J., et al. 2003. Psychiatric symptoms vary with the severity of dementia in probable Alzheimer's disease. J Neuropsych Clin Neurosci. 15(3):346–353. https://doi.org/10.1176/jnp.15.3.346

Lovell, M.A., Ehmann, W.D., Butler, S.M. and Markesbery, W.R. 1995. Elevated thiobarbituric acid-reactive substances and antioxidant enzyme activity in the brain in Alzheimer's disease. Neurology. 45(8):1594–1601. https://doi.org/10.1212/WNL.45.8.1594

Lowry O.H. et al. 1951. Protein measurement with the folin phenol reagent. J Biol Chem. 193:265–275. https://doi.org/10.1016/S0021-9258(19)52451-6

Lu, X.-Y., Huang, S., Chen, Q.-B., Zhang, D., Li, W., Ao, R., et al. 2020. Metformin ameliorates Aβ pathology by insulin-degrading enzyme in a transgenic mouse model of Alzheimer's disease. Oxidative Med Cell Long. 2020. https://doi.org/10.1155/2020/2315106

Lubos, E., Loscalzo, J. and Handy, D.E. 2011. Glutathione peroxidase-1 in health and disease: from molecular mechanisms to therapeutic opportunities. Antioxid Redox Signal. 15(7):1957–1997. https://doi.org/10.1089/ars.2010.3586

Mahdi, O., Chiroma, S.M., Hidayat Baharuldin, M.T., Mohd Nor, N.H., Mat Taib, C.N., Jagadeesan, S., et al. 2021. WIN55, 212-2 attenuates cognitive impairments in AlCl3+ d-Galactose-Induced Alzheimer's disease rats by enhancing neurogenesis and reversing oxidative stress. Biomedicines. 9(9):1270. https://doi.org/10.3390/biomedicines9091270

Mantzavinos, V. and Alexiou, A. 2017. Biomarkers for Alzheimer's disease diagnosis. Curr Alzheimer Res. 14(11):1149–1154. https://doi.org/10.2174/1567205014666170203125942

Martin, J.B. 1999. Molecular basis of the neurodegenerative disorders. N Engl J Med. 340(25):1970–1980. https://doi.org/10.1056/NEJM199906243402507

Moreira, P.I., Carvalho, C., Zhu, X., Smith, M.A. and Perry, G. 2010. Mitochondrial dysfunction is a trigger of Alzheimer's disease pathophysiology. Biochim Biophys Acta (BBA). 1802(1):2–10. https://doi.org/10.1016/j.bbadis.2009.10.006

Nagata, T., Shinagawa, S., Nakajima, S., Noda, Y. and Mimura, M. 2022. Pharmacotherapeutic combinations for the treatment of Alzheimer's disease. Expert Opin Pharmacother. 23(6):727–737. https://doi.org/10.1080/14656566.2022.2042514

Nandi, A., Yan, L.J., Jana, C.K. and Das, N. 2019. Role of catalase in oxidative stress- and age-associated degenerative diseases. Oxid Med Cell Longev. 2019:9613090. https://doi.org/10.1155/2019/9613090

Nguyen, T.K.A., Nguyen, B.N., Hoang, T.M.N., Doan, L.P., Phan, M.G., Lee, H., et al. 2022. Six new polyoxygenated xanthones from garcinia cowa and their neuroprotective effects on glutamate-mediated hippocampal neuronal HT22 cell death. Chem Biodivers. 19(9):e202200376. https://doi.org/10.1002/cbdv.202200376

Nunez, J. 2008. Morris water maze experiment. J Vis Exp. (19). https://doi.org/10.3791/897

Padurariu, M., Ciobica, A., Hritcu, L., Stoica, B., Bild, W. and Stefanescu, C. 2010. Changes of some oxidative stress markers in the serum of patients with mild cognitive impairment and Alzheimer's disease. Neurosci Lett. 469(1):6–10. https://doi.org/10.1016/j.neulet.2009.11.033

Pairojana, T., Phasuk, S., Suresh, P., Huang, S.-P., Pakaprot, N., Chompoopong, S., et al. 2021. Age and gender differences for the behavioral phenotypes of 3xTg Alzheimer's disease mice. Brain Res. 1762:147437. https://doi.org/10.1016/j.brainres.2021.147437

Panichayupakaranant, P. and Sakunpak, A. 2013. Quantitative HPLC analysis of chamuangone in Garcinia cowa leaf extracts. Planta Medica. 79(13):PK29. https://doi.org/10.1055/s-0033-1352289

Piovesan, E.C., Freitas, B.Z.d., Lemanski, F.C.B. and Carazzo, C.A. 2023. Alzheimer's disease: an epidemiological analysis over the number of hospitalizations and deaths in Brazil. Arquivos de Neuro-Psiquiatria. 81(06):577–584. https://doi.org/10.1055/s-0043-1767827

Qiu, C., Kivipelto, M. and Von Strauss, E. 2022. Epidemiology of Alzheimer's disease: occurrence, determinants, and strategies toward intervention. Dialog Clin Neurosci. 11(2):111–128. https://doi.org/10.31887/DCNS.2009.11.2/cqiu

Reed, T.T. 2011. Lipid peroxidation and neurodegenerative disease. Free Radic Biol Med. 51(7):1302–1319. https://doi.org/10.1016/j.freeradbiomed.2011.06.027

Rudan, I., Sidhu, S., Papana, A., Meng, S.J., Xin–Wei, Y., Wang, W. and Sridhar, D. 2015. Prevalence of rheumatoid arthritis in low- and middle-income countries: a systematic review and analysis. J Glob Health. 5(1):010409. https://doi.org/10.7189/jogh.05.010409

Sae-Lim, P., Seetaha, S., Tabtimmai, L., Suphakun, P., Kiriwan, D., Panichayupakaranant, P., et al. 2020. Chamuangone from Garcinia cowa leaves inhibits cell proliferation and migration and induces cell apoptosis in human cervical cancer in vitro. J Pharm Pharmacol. 72(3):470–480. https://doi.org/10.1111/jphp.13216

Sae-Lim, P., Yuenyongsawad, S. and Panichayupakaranant, P. 2019a. Chamuangone-enriched Garcinia cowa leaf extract with rice bran oil: extraction and cytotoxic activity against cancer cells. Pharmacogn Mag. 15(61):183–188. https://doi.org/10.4103/pm.pm_472_18

Sae-Lim, P., Yuenyongsawad, S. and Panichayupakaranant, P. 2019b. Chamuangone-enriched Garcinia cowa leaf extract with rice bran oil: extraction and cytotoxic activity against cancer cells. Pharmacogn Mag. 15(61):183. https://doi.org/10.4103/pm.pm_472_18

Sakunpak, A., Matsunami, K., Otsuka, H. and Panichayupakaranant, P. 2017. Isolation of chamuangone, a cytotoxic compound against Leishmania major and cancer cells from Garcinia cowa leaves and its HPLC quantitative determination method. J Cancer Res Updates. 6(2):38–45. https://doi.org/10.6000/1929-2279.2017.06.02.3

Sakunpak, A. and Panichayupakaranant, P. 2012. Antibacterial activity of Thai edible plants against gastrointestinal pathogenic bacteria and isolation of a new broad spectrum antibacterial polyisoprenylated benzophenone, chamuangone. Food Chem. 130(4):826–831. https://doi.org/10.1016/j.foodchem.2011.07.088

Saleem, U., Chauhdary, Z., Islam, S., Zafar, A., Khayat, R.O., Althobaiti, N. A., et al. 2022. Sarcococca saligna ameliorated D-galactose induced neurodegeneration through repression of neurodegenerative and oxidative stress biomarkers. Metab Brain Dis. 38:717–734. https://doi.org/10.1007/s11011-022-01046-w

Saleem, U., Chauhdary, Z., Raza, Z., Shah, S., Rahman, M.-u., Zaib, P., et al. 2020. Anti-Parkinson's activity of tribulus terrestris via modulation of AChE, α-Synuclein, TNF-α, and IL-1β. ACS Omega. 5(39):25216–25227. https://doi.org/10.1021/acsomega.0c03375

Saleem, U., Shehzad, A., Shah, S., Raza, Z., Shah, M.A., Bibi, S., et al. 2021. Antiparkinsonian activity of Cucurbita pepo seeds along with possible underlying mechanism. Metab Brain Dis. 36:1231–1251. https://doi.org/10.1007/s11011-021-00707-6

Schliebs, R. and Arendt, T. 2006. The significance of the cholinergic system in the brain during aging and in Alzheimer's disease. J Neural Transm. 113:1625–1644. https://doi.org/10.1007/s00702-006-0579-2

Sharma, P., Tripathi, A., Tripathi, P.N., Prajapati, S.K., Seth, A., Tripathi, M. K. and Shrivastava, S.K. 2019. Design and development of multitarget-directed N-Benzylpiperidine analogs as potential candidates for the treatment of Alzheimer's disease. Eur J Med Chem. 167:510–524. https://doi.org/10.1016/j.ejmech.2019.02.030

Shin, I.-S., Carter, M., Masterman, D., Fairbanks, L. and Cummings, J.L. 2005. Neuropsychiatric symptoms and quality of life in Alzheimer's disease. Am J Geriatr Psychiatry. 13(6):469–474. https://doi.org/10.1097/00019442-200506000-00005

Singh, N.A., Bhardwaj, V., Ravi, C., Ramesh, N., Mandal, A.K.A. and Khan, Z.A. 2018. EGCG nanoparticles attenuate aluminum chloride-induced neurobehavioral deficits, beta amyloid and tau pathology in a rat model of Alzheimer's disease. Front Aging Neurosci. 10:244. https://doi.org/10.3389/fnagi.2018.00244

Sisodia, S.S. 1999. Series introduction: Alzheimer's disease: perspectives for the new millennium. J Clin Invest. 104(9):1169–1170. https://doi.org/10.1172/JCI8508

Sultana, R., Perluigi, M. and Butterfield, D.A. 2013. Lipid peroxidation triggers neurodegeneration: a redox proteomics view into the Alzheimer's disease brain. Free Radic Biol Med. 62:157–169. https://doi.org/10.1016/j.freeradbiomed.2012.09.027

Tran, D., Nguyen, H., Pham, T., Nguyen, A.T., Nguyen, H.T., Nguyen, N.B., et al. 2022. Resources for enhancing Alzheimer's caregiver health in Vietnam (REACH VN): exploratory analyses of outcomes of a cluster randomized controlled trial to test the feasibility and preliminary efficacy of a family dementia caregiver intervention in Vietnam. Am J Geriatr Psychiatry. 30(8):878–882. https://doi.org/10.1016/j.jagp.2022.04.011

Tran, M. and Reddy, P. H. 2021. Defective autophagy and mitophagy in aging and Alzheimer's disease. Front Neurosci. 14:612757. https://doi.org/10.3389/fnins.2020.612757

Ulep, M.G., Saraon, S.K. and McLea, S. 2018. Alzheimer disease. J Nurse Pract. 14(3):129–135. https://doi.org/10.1016/j.nurpra.2017.10.014

Vorhees, C.V. and Williams, M.T. 2006. Morris water maze: procedures for assessing spatial and related forms of learning and

memory. Nature Protoc. 1(2):848–858. https://doi.org/10.1038/nprot.2006.116

Walf, A.A. and Frye, C.A. 2007. The use of the elevated plus maze as an assay of anxiety-related behavior in rodents. Nature Protoc. 2(2):322–328. https://doi.org/10.1038/nprot.2007.44

Winslow, B.T., Onysko, M.K., Stob, C.M. and Hazlewood, K.A. 2011. Treatment of Alzheimer disease. Am Fam Physician. 83(12):1403–1412.

Xing, Z., He, Z., Wang, S., Yan, Y., Zhu, H., Gao, Y. and Zhang, L. 2018. Ameliorative effects and possible molecular mechanisms of action of fibrauretine from Fibraurea recisa Pierre on d-galactose/AlCl 3-mediated Alzheimer's disease. RSC Adv. 8(55):31646–31657. https://doi.org/10.1039/C8RA05356A

Yiannopoulou, K.G. and Papageorgiou, S.G. 2013. Current and future treatments for Alzheimer's disease. Therap Adv Neurolog Disord. 6(1):19–33. https://doi.org/10.1177/1756285612461679

Yiannopoulou, K.G. and Papageorgiou, S.G. 2020. Current and future treatments in Alzheimer disease: an update. J Cent Nerv Syst Dis. 12:1179573520907397. https://doi.org/10.1177/1179573520907397

Yin, S., Ran, Q., Yang, J., Zhao, Y. and Li, C. 2020. Nootropic effect of neferine on aluminium chloride-induced Alzheimer's disease in experimental models. J Biochem Mol Toxicol. 34(2):e22429. https://doi.org/10.1002/jbt.22429

Yorsin, S., Sriwiriyajan, S. and Chongsa, W. 2023. Vasorelaxing effect of Garcinia cowa leaf extract in rat thoracic aorta and its underlying mechanisms. J Trad Complement Med. 13(3):219–225. https://doi.org/10.1016/j.jtcme.2022.12.001

Zhang, Z., Zhang, Q., Xue, Y., Fang, H. and Wu, Z. 2023. Serum levels of reduced glutathione, oxidized glutathione, and glutathione reductase activity in minor recurrent aphthous stomatitis patients. J Dent Sci. 18(3):1103–1108. https://doi.org/10.1016/j.jds.2022.11.016

Supplementary

Table S1. Tabular Data.

Open field test						
Groups	**Control**	**Disease control**	**Standard**	**2.5 mg/kg**	**5.0 mg/kg**	**7.5 mg/kg**
Total number of square crossing (Figure 1)	52.0 ± 0.57	15 ± 0.68$^{###}$	48 ± 0.69***	24 ± 0.76***	35.0 ± 0.75***	49 ± 0.61***
Peripheral exploration numbers (Figure 2)	143 ± 0.50	43 ± 0.65$^{###}$	102 ± 0.57***	56 ± 0.69***	68 ± 0.67***	105 ± 0.65***
Central exploration numbers (Figure 3)	99 ± 0.55	35 ± 0.73$_{###}$	101 ± 0.72***	52 ± 0.53***	64 ± 0.79***	84 ± 0.57***
Morris water maze test/escape latency (Figure 4)						
Day 39	40 ± 0.71	58 ± 0.75$^{###}$	57 ± 0.72***	59 ± 0.57***	56 ± 0.65***	55 ± 0.68***
Day 40	39 ± 0.69	51 ± 0.67$^{###}$	46 ± 0.63ns	48 ± 0.58***	49 ± 0.57***	45 ± 0.53***
Day 41	35 ± 0.57	31 ± 0.71$^{###}$	37 ± 0.67 ns	37 ± 0.61***	34 ± 0.69***	32 ± 0.75***
Day 42	20 ± 0.66	28 ± 0.57$^{###}$	19 ± 0.53***	25 ± 0.54 ns	22 ± 0.57***	16 ± 0.61***
Y-maze task						
Number of triads (Figure 5)	8 ± 0.57	2 ± 0.59$^{###}$	6 ± 0.56***	3 ± 0.57*	4 ± 0.59*	7 ± 0.75***
Number of arm entries (Figure 6)	70 ± 0.52	15 ± 0.70$^{###}$	65 ± 0.75***	20 ± 0.75***	30 ± 0.61***	50 ± 0.59***
Spontaneous alterations (%) (Figure 7)	11 ± 0.53	2 ± 0.77$^{###}$	9 ± 0.56***	5 ± 0.60***	8 ± 0.58*	10 ± 0.78***
Elevated maze test						
Transfer latency (Figure 8)	24 ± 0.67	74 ± 0.76$^{###}$	34 ± 0.73***	78 ± 0.87**	62 ± 0.67***	42 ± 0.58***